

Cyclotron resonance harmonics in the organic superconductor β'' -(BEDT-TTF) $_2$ SF $_5$ CH $_2$ CF $_2$ SO $_3$; observation of a new kind of effective mass renormalization

R.S. Edwards, J.A. Symington, A. Ardavan, J. Singleton, E. Rzepniewski, and R.D. McDonald
Department of Physics, University of Oxford, The Clarendon Laboratory, Parks Road, Oxford, OX1 3PU, U.K.

J. Schlueter and A.M. Kini
*Chemistry and Materials Divisions, Argonne National Laboratory,
 9700 South Cass Avenue, Argonne, Illinois, U.S.A.*

Cyclotron resonance, along with its second and third harmonics, has been observed in the quasi-two-dimensional organic superconductor β'' -(BEDT-TTF) $_2$ SF $_5$ CH $_2$ CF $_2$ SO $_3$. The harmonic content is richly angle-dependent, and is interpreted in terms of the interlayer warping of the Fermi surface giving rise to the cyclotron resonance. In a departure from Kohn's theorem, but in agreement with recent theoretical predictions, the effective mass deduced from the cyclotron resonance measurements is greater than that determined from magnetic quantum oscillations.

PACS numbers: 71.27, 71.18, 71.20.Rv, 72.80.Le, 74.70.Kn

Many correlated-electron systems which are of fundamental or technological interest have very anisotropic electronic bandstructure. Examples include the "high- T_c " cuprates [1], layered phases of the manganites [2] and ruthenates [3], semiconductor superlattices [4] and crystalline organic metals [5, 6]. Such systems are often characterised by a tight-binding Hamiltonian in which the ratio of the interlayer transfer integral t_\perp to the average intralayer transfer integral t_\parallel is much less than 1. The resulting highly anisotropic dispersion relationships have been shown to give rise to a range of interesting d.c. and a.c. angle-dependent magnetoresistance oscillation (AMRO) effects [6].

In this paper we describe an experiment demonstrating a new effect of this kind, the variation with magnetic field orientation of the harmonic content of cyclotron resonance (CR) measured in the high-frequency interlayer conductivity. The effect arises because the interlayer velocity component of a quasiparticle that executes a cyclotron orbit around a warped cylindrical Fermi surface (FS) section acquires higher harmonic content as the steady magnetic field causing the orbit is tilted away from the cylinder axis. It may be considered a high-frequency analogue of the Yamaji effect, in which the d.c. magnetoresistance oscillates as a function of magnetic field orientation.

In a detailed study of the d.c. AMRO of the quasi-two-dimensional (Q2D) organic molecular metal β'' -(BEDT-TTF) $_2$ SF $_5$ CH $_2$ CF $_2$ SO $_3$ [7], we use the Yamaji oscillations to parameterize the shape and orientation of the Q2D FS of this material. Then, for the first time in any material the detailed angle-dependence of the harmonic content of CR is examined, and we verify the form of the Fermi surface, demonstrating that this effect could form the basis of a new technique for studying the Fermi surface topology of low-dimensional materials. The CR measurements also exhibit a mass renormalisation effect recently predicted to occur in narrow-bandwidth metallic

systems [8].

Experiments were carried out on single crystals ($\sim 0.5 \times 0.5 \times 0.1$ mm 3) prepared by electrocrystallisation [7]. Samples were initially orientated using infrared reflectivity [9] to $\pm 4^\circ$. For d.c. measurements, electrical contacts were made to the upper and lower faces (parallel to the **ab** (Q2D) planes) of selected crystals by attaching 25 μ m Au wires using graphite paint (contact resistances $\lesssim 10$ Ω). The resistance was measured by driving a low-frequency a.c. current (5 μ A, 17 – 200 Hz) in the **c*** (interlayer) direction; the voltage was measured in the **c*** direction using a lock-in amplifier. In this configuration, the resistance is proportional to the interplane resistivity component ρ_{zz} [6]. Samples were mounted in a cryostat providing temperatures T between 0.50 K and 4.2 K, and allowing rotation about two mutually perpendicular axes. The sample's angular coordinates are the angle θ between the magnetic field **B** and **c*** and the angle ϕ defining the plane of rotation [6, 10].

Fig. 1(a) shows the θ, ϕ dependence of the magnetoresistance for $B = 10$ T and $T = 1.5$ K. The data show AMROs with sharp maxima (the Yamaji effect), suggesting that they are due to a Q2D FS section, rather than open sheets [6, 10]. (For all ϕ , a sharp dip is visible at $\theta = 90^\circ$ as the superconducting upper critical field becomes large when **B** is parallel to the Q2D layers, causing a reduction in ρ_{zz} . See Ref. [11] for a discussion.) Such AMRO maxima occur at angles θ_n given by $c'k_\parallel \tan(\theta_n) = \pi(n \pm \frac{1}{4}) + f(\phi)$, where c' is the effective interplane spacing, n is an integer, k_\parallel is the maximum Fermi wave-vector in the plane of rotation and $f(\phi)$ is a function of the plane of rotation of the field [6, 10]. The + and – signs correspond to $\theta_n > 90^\circ$ and $\theta_n < 90^\circ$ respectively. The ϕ dependence of the AMRO data is most accurately fitted by a non-elliptical FS cross section [10], $(\frac{k_x}{k_a})^j + (\frac{k_y}{k_b})^j = 1$. A free-parameter fit yielded $j = 1.1 \pm 0.1$ and a ratio $k_a/k_b = 9.0 \pm 0.2$, leading to the "diamond-shaped" FS shown in Fig. 1(b); the

FS long axis makes an angle of $68 \pm 4^\circ$ with the \mathbf{b}^* axis of the crystal. The fitted FS cross-section has an area corresponding to a de Haas-van Alphen (dHvA) frequency of $F = 196 \pm 3$ T, in excellent agreement with Shubnikov-de Haas (SdH) and dHvA studies which yield $F = 200 \pm 1$ T [12]. The disagreement between the area deduced from AMRO and the dHvA experiments was significantly worse if the FS cross-section was constrained to be elliptical ($j = 2$) [12]. Swept-field magnetotransport measurements were also carried out at fixed θ, ϕ over a range of T . A $\theta = 0$ effective mass m^* of $1.96 \pm 0.05 m_e$ was obtained by fitting the T -dependence of small-amplitude $F = 200$ T SdH oscillations to the 2D Lifshitz-Kosevich theory [6], in good agreement with previous studies [12].

The CR measurements were made using resonant cavity techniques [13]. A β'' -(BEDT-TTF) $_2$ SF $_5$ CH $_2$ CF $_2$ SO $_3$ sample was placed inside a rectangular cavity resonating in the TE $_{102}$ mode at 71.2 GHz [13]. Samples were aligned in the cavity such that the oscillating \mathbf{H} field was parallel to the Q2D planes; induced currents flow in the interplane (low-conductivity) direction, leading to a skin depth greater than the sample dimensions [13, 14] and dissipation dominated by the interplane conductivity [13, 14, 16]. The cavity can be rotated with respect to \mathbf{B} , thus changing θ without changing the electromagnetic environment of the sample in the cavity. The sample can also be rotated inside the cavity to change ϕ . Quasi-static fields were provided by a superconductive magnet in Oxford and by a 33 T Bitter magnet at NHMFL, Tallahassee.

Field sweeps were carried out at various θ for $\phi = 105^\circ, 75^\circ, 45^\circ$ and 15° . Fig. 2 shows field sweeps between 0 and 15 T at a fixed frequency of 71.2 GHz, for $\phi = 105^\circ$ and 45° . Only θ angles between 0 and 70° are shown, as the resonance positions are symmetrical about $\theta = 0$. The data have been normalised and offset for clarity. The feature at 2 T on all sweeps is a background of the apparatus [13]. At intermediate fields, broad resonances can be seen. For $\phi = 105^\circ$, one resonance moves to higher fields with increasing angle. The position of the resonance in magnetic field for different θ is fitted to $\frac{\omega}{B} = A \cos(\theta - \theta_0)$ [6], giving values $A/\omega = 0.175 \pm 0.005$ T $^{-1}$ and $\theta_0 = 2^\circ \pm 2^\circ$. This is consistent with the behaviour expected of a CR, where the resonance should be centred on $\theta_0 = 0^\circ$ [6].

At $\phi = 45^\circ$ (Fig. 2(b)) a second resonance also appears for higher θ at approximately half the field of the main CR. This resonance is also seen for $\phi = 75^\circ$ and $\phi = 15^\circ$, and also follows a $\cos \theta$ dependence of $1/B$ with fitting parameters $A/\omega = 0.36 \pm 0.01$ T $^{-1}$ and $\theta_0 = -1^\circ \pm 1^\circ$. The value of A/ω strongly suggests that this resonance is the second harmonic of the main CR. At some azimuthal angles an additional feature becomes visible at $\theta \sim 60^\circ$, behaving like a third harmonic of the CR.

Ref. [15] predicts the presence of harmonics in the real space velocity of charge carriers in cyclotron orbits about non-elliptical FS cross-sections, leading to harmonics of

the CR. It does not, however, predict even harmonics for a symmetrical FS such as that in Fig. 1(b). By contrast, Hill [16] considers a cylindrical FS which is warped in the interplane direction, in which the warping vector is *not* directed along the cylinder axis. Harmonics of the CR are predicted, but the model is unable to reproduce the behaviour reported here. Instead we propose a mechanism which predicts CR harmonics and their angular behaviour without the need for a shifted warping vector. Fig. 2(c) shows the cross section of a warped Q2D FS section (warping greatly exaggerated). For a general orientation of \mathbf{B} , quasiparticles follow orbits about the FS such that the z -component of their real space velocity, v_z oscillates (the velocity is always perpendicular to the FS [6]). In our measurement geometry, the dissipation caused by the sample is dominated by interplane currents, i.e. by the behaviour of v_z [13, 14]. If θ is small, the orbits remain within the length of one Brillouin zone (BZ) in the k_z -direction and v_z oscillates at the cyclotron frequency ω_c . As θ increases, the orbits extend over several BZs in the k_z direction and v_z acquires oscillatory components at harmonics of ω_c . (Note that the precise harmonic content depends on the average k_z of the orbit; the conductivity depends on an average over all possible orbits [13, 14].) The largest amplitude of the ω_c resonance will occur at angle θ_1 in Fig. 2(c), as the change in v_z during an orbit will be greatest for all possible orbits. The second harmonic will likewise be strongest at θ_2 , and at θ_p for the p th harmonic. Simple geometry leads to

$$\tan \theta_1 \approx \pi/ck_F; \quad \tan \theta_p \approx p\pi/ck_F, \quad (1)$$

where $2\pi/c$ is the height of the BZ in the interlayer direction and $2k_F$ is the average width of the FS cross-section in the plane of rotation of \mathbf{B} . Fig. 3(a) shows the intensity of the resonances at $\phi = 75^\circ$ as a function of θ . The θ dependence of the resonance intensity has been fitted to a suitable functional form [17] centred on θ_1 . The angular behaviour of the second and third harmonics has then been predicted using the same function, but centred on θ_2 and θ_3 respectively.

The angle θ_1 depends on the anisotropy of the FS and its orientation. Figs. 2(c) and (d) represent rotating the field through the major and minor axes of the FS cross-section. In Fig. 2(d), θ_1 is much higher than for (c). θ_1 should vary with rotation as

$$\theta_1 = C + D \cos 2(\phi + \phi_0), \quad (2)$$

where ϕ_0 is related to the orientation of the FS with respect to the crystal axes and C and D are constants corresponding to the major and minor axes of the FS cross-section. Fig. 3(b) shows the values of θ_1 for the ϕ -orientations studied fitted to Eqn. 2. From the maximum and minimum values of θ_1 the major and minor axes of the FS cross-section are found to be in the ratio $10.5 \pm 1.8:1$, in good agreement with the $9 \pm 0.2:1$ found from the AMRO data. The fitted value of ϕ_0 is used to orientate the FS with respect to the crystal axes, as shown in Fig.

3(b, inset). The orientation of the major axis (at $68 \pm 4^\circ$ to the \mathbf{b}^* axis) agrees with orientations deduced from the current and previous AMRO data [10, 12] (also $68 \pm 4^\circ$).

A cyclotron mass $m_{\text{CR}}^* = 2.3 \pm 0.1 m_e$ was deduced from the angular frequency ω and field B of the fundamental CR at $\theta = 0$ using $\omega = eB/m_{\text{CR}}^*$ [6]. CR gives a measure of the quasiparticle mass different from that given by thermodynamic experiments such as the dHvA effect [6, 18]. In the simplest picture [6, 18], the mass measured in CR represents the bare band mass renormalised by electron-phonon interactions, whereas the mass m^* measured using quantum oscillatory techniques is additionally renormalised by electron-electron interactions. In spite of a large number of experiments on BEDT-TTF salts (see Ref. [6] for details), only two definitive reports of CR, both in α -(BEDT-TTF) $_2$ NH $_4$ Hg(SCN) $_4$, have been made [16, 19]. In these studies, a CR mass of $m_{\text{CR}}^* = 1.9 m_e$ was measured [16, 19]; this may be compared with $m^* = 2.5 m_e$ [20]. The relative sizes of the two masses ($m_{\text{CR}}^* < m^*$) is therefore in agreement with the above predictions. By contrast, in the current experiments on β'' -(BEDT-TTF) $_2$ SF $_5$ CH $_2$ CF $_2$ SO $_3$, $m^* = 1.96 \pm 0.05 m_e$ and $m_{\text{CR}}^* = 2.3 \pm 0.1 m_e$; *i.e.* $m_{\text{CR}}^* > m^*$. Thus it appears that the predictions of an enhancement of the effective mass derived from quantum oscillations over that in a CR-like experiment do not necessarily hold and that Kohn's the-

orem [21] is violated. Hubbard-model calculations have recently been carried out [8] which contradict the simple theories and appear to support the current experimental data. In these calculations it was found that the relationship between the two masses depends strongly on the characteristics of the material measured (e.g. band filling) and in some cases m^* can be exceeded by m_{CR}^* .

In summary, we have performed experiments on β'' -(BEDT-TTF) $_2$ SF $_5$ CH $_2$ CF $_2$ SO $_3$, showing that the Q2D section of the Fermi surface (FS) is highly elongated and non-elliptical. Harmonics of cyclotron resonance (CR) have been observed and are explained by a mechanism which confirms the elongation and orientation of the FS cross-section. The method is consistent with a FS which is extended in the interlayer direction, giving strong support for coherent interlayer charge-transfer in this material. We have also found that the effective mass from CR experiments is greater than that measured by magnetic quantum oscillations, in agreement with recent theoretical work and in violation of Kohn's theorem.

This work is supported by EPSRC (UK). NHMFL Tallahassee is supported by the US Department of Energy (DoE), NSF and the State of Florida. Work at Argonne is sponsored by the DoE, Office of Basic Energy Sciences, Division of Materials Science under contract number W-31-109-ENG-38.

-
- [1] L.B. Ioffe and A.J. Millis, *Science* **285**, 1241 (2000).
 [2] C.N.R. Rao *J. Mater. Chem.* **9**,1 (1999).
 [3] C. Bergemann *et al.*, *Phys. Rev. Lett.* **84**, 2662 (2000).
 [4] M.J. Kelly, *Low dimensional semiconductors* (Oxford University Press 1995).
 [5] S.P. Strong *et al.* *Phys. Rev. Lett.* **73**, 1007 (1994)
 [6] J. Singleton, *Reports on Progress in Physics* **63**, 1111 (2000).
 [7] U. Geiser *et al.* *J. Am. Chem. Soc.* **118**, 9996 (1996).
 [8] K.Kanki and K. Yamada, *J. Phys. Soc. Jpn.* **66**, 1103 (1997).
 [9] J. Dong *et al.* *Phys. Rev. B* **60**, 4342 (1999).
 [10] M.-S. Nam *et al.* *J. Phys.: Condens. Matter*, in press.
 [11] J. Singleton *et al.* *J. Phys.: Condens Matter* **12** L641 (2000).
 [12] J. Wosnitzer *et al.*, *Synth. Met.* **103**, 2000 (1999); *Phys. Rev. B* **61**, 7383 (2000).
 [13] A. Ardavan *et al.*, *Phys. Rev. Lett.* **81**, 713 (1998).
 [14] Stephen Hill, *Phys. Rev. B* **62**, 8699 (2000)
 [15] S.J. Blundell *et al.* *Phys. Rev. B* **55**, 6129 (1997).
 [16] S. Hill, *Phys. Rev. B* **55**, 4931 (1997).
 [17] R.S. Edwards *et al.*, to be published. For practical purposes, the function is close to a Gaussian in $\tan \theta$.
 [18] K.F. Quader *et al.* *Phys. Rev. B* **36**, 156 (1987); A.J. Leggett, *Annals of Physics* **46**, 76 (1968); W. Kohn, *Phys. Rev.* **123**, 1242 (1961).
 [19] A. Polisskii *et al.* *J. Phys: Condens. Mat.* **8**, L195 (1996)
 [20] M. D'operto *et al.* *Phys. Rev. Lett.*, **69**, 991 (1992).
 [21] Kohn's theorem states that the effects of electron-electron interactions are not observed in a millimetre-wave measurement of cyclotron resonance; see W. Kohn, *Phys. Rev.* **123** 1242 (1961).

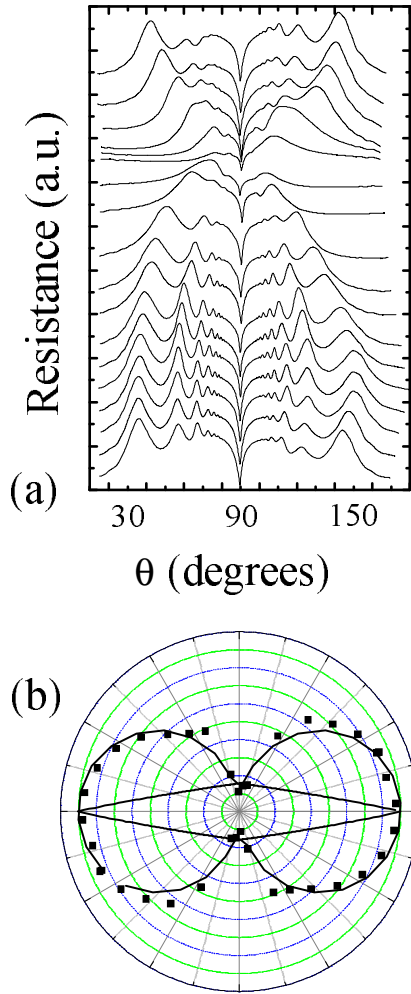


FIG. 1: (a) AMRO data for β'' -(BEDT-TTF) $_2$ SF $_5$ CH $_2$ CF $_2$ SO $_3$ at 10 T and 1.5 K for ϕ -angles $7 \pm 1^\circ$ (top trace) $17 \pm 1^\circ$, $27 \pm 1^\circ$, $177 \pm 1^\circ$ (bottom trace- adjacent traces spaced by $10 \pm 1^\circ$). $\phi = 0$ corresponds to rotation in the $\mathbf{a}^* \mathbf{c}^*$ plane of the crystal to within the accuracy of the infrared orientation. (b) The ϕ dependence of k_{\parallel} from the $\tan \theta$ periodicity of the AMRO in Fig. 1(a) (points); the “figure of eight” solid curve is a fit. The resulting fitted FS pocket (elongated diamond shape; $j = 1.1$) is shown within. The long axis of the pocket makes an angle of $68 \pm 4^\circ$ with the \mathbf{b}^* axis.

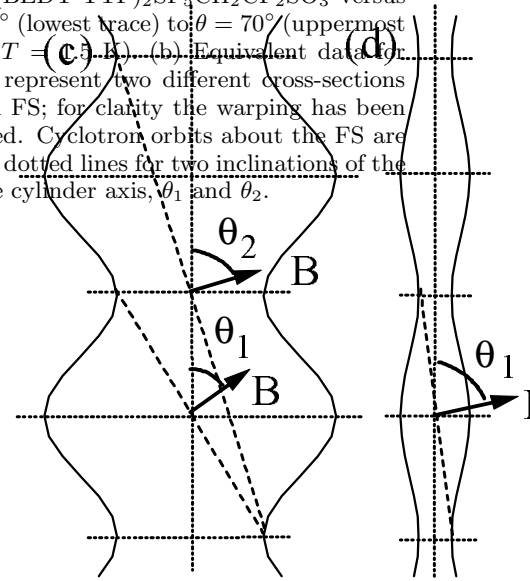
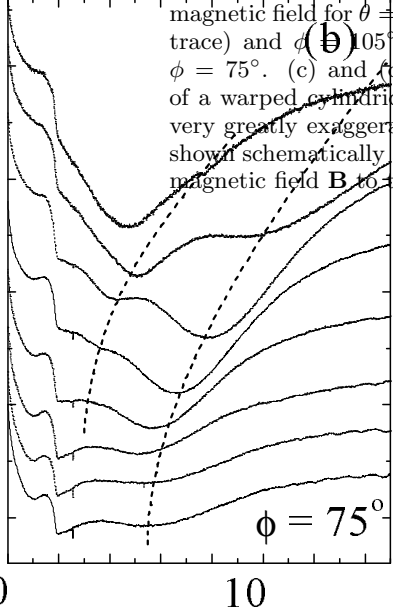
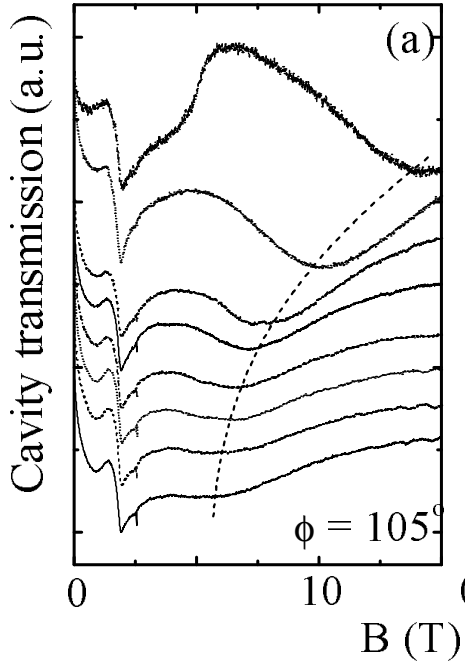


FIG. 2: (a) Transmission of the resonant cavity loaded with a single crystal of β'' -(BEDT-TTF) $_2$ SF $_5$ CH $_2$ CF $_2$ SO $_3$ versus magnetic field for $\theta = 0^\circ$ (lowest trace) to $\theta = 70^\circ$ (uppermost trace) and $\phi = 105^\circ$ ($T = 4.5$ K). (b) Equivalent data for $\phi = 75^\circ$. (c) and (d) represent two different cross-sections of a warped cylindrical FS; for clarity the warping has been very greatly exaggerated. Cyclotron orbits about the FS are shown schematically as dotted lines for two inclinations of the magnetic field B to the cylinder axis, θ_1 and θ_2 .

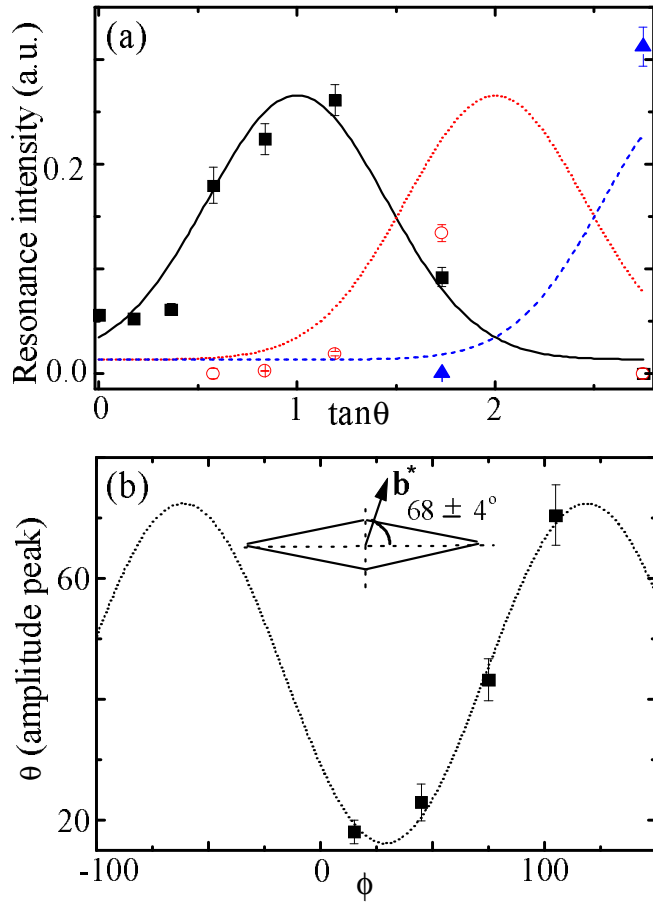


FIG. 3: (a) Intensity of CRs versus $\tan\theta$ for $\phi = 75^\circ$. Solid curve: fit to the intensity of the fundamental CR, giving angle θ_1 (data: square points). Dotted curve: predicted intensity of the second harmonic, centred on θ_2 (data: hollow circles). Dashed curve: predicted intensity of the third harmonic, centred on θ_3 (data: triangles). (b) θ_1 versus ϕ ; points: experimental values; the curve is a fit to Equation 2. Inset: the orientation of the FS cross-section at $68 \pm 4^\circ$ to the crystal's \mathbf{b}^* axis derived from the fit.